Journal of Physics: Conference Series **688** (2016) 012020 doi:10.1088/1742-6596/688/1/012020

High-Energy Density science at the Linac Coherent Light Source

S H Glenzer, L B Fletcher, and J B Hastings
SLAC National Accelerator Laboratory, 2575 Sand Hill Road, MS 19, Menlo Park, CA 94025

E-mail: glenzer@slac.stanford.edu

Abstract. The Matter in Extreme Conditions end station at the Linac Coherent Light Source holds great promise for novel pump-probe experiments to make new discoveries in high-energy density science. In recent experiments we have demonstrated the first spectrally-resolved measurements of plasmons using a seeded 8-keV x-ray laser beam. Forward x-ray Thomson scattering spectra from isochorically heated solid aluminum show a well-resolved plasmon feature that is down-shifted in energy by 19 eV from the incident 8 keV elastic scattering feature. In this spectral range, the simultaneously measured backscatter spectrum shows no spectral features indicating observation of collective plasmon oscillations on a scattering length comparable to the screening length. This technique is a prerequisite for Thomson scattering measurements in compressed matter where the plasmon shift is a sensitive function of the free electron density and where the plasmon intensity provides information on temperature.

1. Introduction

With the advent of the Linac Coherent Light Source (LCLS) x-ray laser [1] and the commissioning of the Matter of Extreme Conditions (MEC) end station [2] an unprecedented experimental capability has become available to explore extreme matter conditions with accurate pump-probe measurements [3], cf., Fig.1. Experiments that apply spectrally resolved x-ray scattering to probe plasma conditions of compressed solids offer novel techniques to determine the physical properties of matter at mega bar pressures. The ultrafast temporal resolution provided by the LCLS x-ray source and the high repetition rate of these experiments makes studies of high-pressure phase transitions [4,5], observations of novel structural properties [6], or direct measurements of material strain rates highly attractive.

For this purpose, the MEC instrument is equipped with one ultra-short pulse laser and two nanosecond laser beams that drive the material into extreme matter conditions, for example, by isochoric heating or by launching shock waves that propagate through solid foil targets. In these conditions, spectrally resolved x-ray Thomson scattering measurements in the non-collective (backward) scattering regime provide information of the microscopic physics by measuring the free electron distribution function. On the other hand, in the collective (forward) scattering regime, plasmon (Langmuir) [7-9] or ion acoustic oscillations are observed [10]. In particular, the plasmon scattering spectrum is of fundamental interest because it holds promise to determine plasma parameters and the physical properties from first principles [11]. This is particularly relevant for solid densities and above where

the plasma is often closely coupled and standard theoretical approximations that have been developed for solids or ideal plasmas are not applicable. On the other hand, knowledge of dense plasma conditions are important for warm dense matter studies and potential future applications where contemporary physics pursues questions related to particle acceleration, inertial confinement fusion, and laboratory astrophysics.

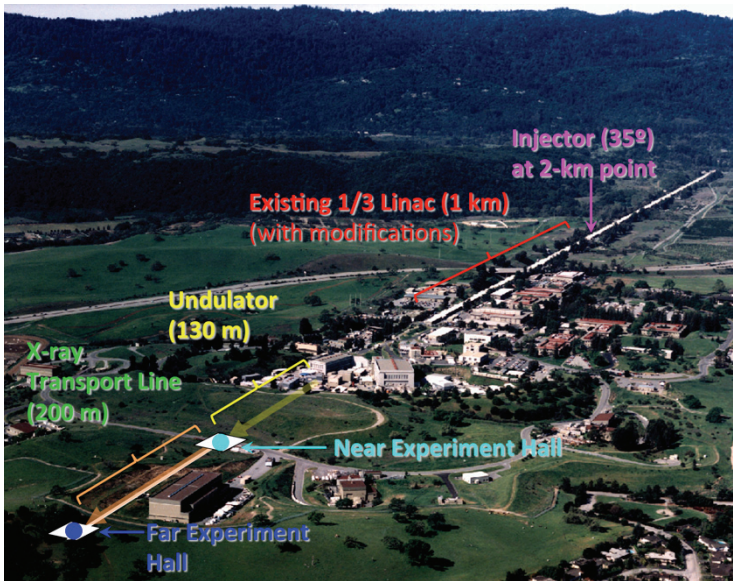

Figure 1. Areal view of the Linac Coherent Light Source. Electrons are injected at the 2 km point of the Linac that accelerates electron bunches over 1 km to energies ranging from 4.3 to 14 GeV. A 130 m long undulator is then producing the Free Electron Laser (FEL) x-ray beam with energies ranging from 1.5 Å to 15 Å at 120 Hz for experiments in the near and far experimental halls. The MEC is the 3rd instrument in the far experimental hall that is reached after a 200 m-long x-ray transport line. At MEC, the x-ray beam can deliver x-ray energies from 480 to 10,000 eV with pulse durations of 5 to 500 fs and up to 4 mJ FEL pulse energy.

LCLS provides a powerful penetrating x-ray beam with unique properties to probe the conditions in these short-lived hot dense states of matter. The beam delivers approximately 10^{12} x-ray photons in a micron-scale focal spot allowing measurements with high spectral resolution of $\Delta E/E = 10^{-4}$ (in a seeded beam mode [12]), high wave-number resolution of $\Delta k/k = 10^{-2}$, and high temporal resolution of 20-50 fs. Consequently, by employing highly efficient curved crystal spectrometers, the plasmon spectrum can be observed in single shots.

In this study, experiments have been performed in single shot mode and at high repetition rate of 115 Hz. The latter allowed us to measure quasi noise-free plasmon spectra within 7 seconds that determine the plasmon dispersion and intensity for warm solid-density aluminum. The plasmon shift of 19 eV yields $n_e = 1.8 \times 10^{23}$ cm^{-3} expected for Z = 3 and temperatures less than 1 eV. These findings demonstrate the plasmon scattering capability at LCLS and will motivate future investigations in hot compressed matter.

2. X-ray Thomson scattering in dense plasmas

The x-ray scattering process is markedly different from optical scattering as the energy of the incident x-ray photon with frequency w_0 is large enough to give a significant Compton or plasmon shift to the frequency of the scattered radiation. During the scattering process, the incident photons transfer the momentum $h\mathbf{k}/2\pi$ and the energy $hw_C/2\pi = (h\mathbf{k}/2\pi)^2/2m_e$ to the electrons. The magnitude of the **k**-vector is given by

$$k = |\mathrm{k}| = \frac{4\pi hc}{E_0}\sin\left(\frac{\theta}{2}\right) \qquad (1)$$

with $E_0 = hw_0/2\pi$ being the energy of the probe x rays and θ the scattering angle. Momentum and energy is transferred to free electrons and to electrons whose binding energy is less than $hw_C/2\pi$. With the scattering vector defined by x-ray energy and scattering geometry, the Thomson scattering regime

is characterized by the scattering parameter α that is proportional to the ratio of the x-ray probe scale-length to the plasma screening length, λ_S:

$$\alpha = \frac{1}{k\lambda_S} \tag{2}$$

For $\alpha < 1$, the non-collective regime, spectrally-resolved incoherent Thomson scattering measures the momentum distribution function for free electrons, and hence the electronic temperature. In warm dense matter, however, this spectrum blends with the bound-free scattering spectrum [13-15] that measures the momentum distribution of the bound electrons. Moreover, bound electrons with ionization energies larger than $\hbar w_C/2\pi$ (states deep in the Fermi sphere) cannot be excited, and no energy can be transferred during the scattering process giving rise to an elastic scattering feature. For $\alpha > 1$, the collective scattering regime, the scattering is sensitive to temporal and spatial correlations between electron motion separated by a screening length, and therefore observes ion-acoustic and electron plasma wave resonances.

The total scattering spectrum results in elastic and inelastic spectral features that are calculated with the dynamic form factor. The free electron contribution is described by $S_{ee}(\boldsymbol{k},\omega)$, while the un-shifted elastic scattering component at E_0 that is commonly referred to as Rayleigh peak is described by the first term of the dynamic structure factor [16-17]

$$S(k,\omega) = \left|f_I(k) + q(k)\right|^2 S_{ii}(\mathrm{k}) + Z_f S_{ee}(k,\omega) + Z_c \int S_{CE}(k,\omega-\omega')S_S(k,\omega')d\omega' \tag{3}$$

with Z_f and Z_C the number of free and bound electrons, respectively. The last term of Eq. (3) calculates the bound-free scattering contribution. This expression for the dynamic structure factor allows a few simple approximations. Of interest to this study, $\alpha > 1$ results in collective scattering and the plasmon frequency shift from E_0 is determined by the plasmon dispersion relation and the width is determined by Landau damping and collisional damping processes. The shift can be approximated for small values of k using an inversion of Fermi integrals given by Zimmerman [18] that results in a modified Bohm-Gross dispersion relation [18-19]

$$\omega_{pl}^2 = \omega_p^2 + 3k^2 v_{th}^2\left(1 + 0.088 n_e \Lambda_e^3\right) + \left(\frac{\hbar k^2}{2m_e}\right)^2 \tag{4}$$

where $\omega_p = \sqrt{n_e e^2/\varepsilon_0 m_e}$ is the plasma frequency, $v_{th} = \sqrt{k_B T_e/m_e}$ is the thermal velocity, and $\Lambda_e = h/\sqrt{2\pi m_e k_B T_e}$ is the thermal wavelength. For solid-density plasma conditions encountered in warm dense matter, Eq. (4) results in energy shifts in the range of 15 – 50 eV consequently requiring a high-energy x-ray source of $E > 3$ keV and $\Delta E/E = 10^{-3}$ - 10^{-4} to both penetrate through the dense plasma and to resolve the plasmon frequency shift. Furthermore, it is noteworthy to realize that simultaneous energy resolution of $\Delta E/E < 10^{-4}$ and wavenumber resolution of $\Delta k/k < 10^{-1}$ will be needed to resolve plasmon broadening determined by damping processes in the plasma.

3. Results and Discussions

In this study, we first validated plasmon measurements at high repetition rate with high-resolution measurements of isochorically heated targets before applying the technique in single shots on shock-compressed aluminum. Figure 4 shows the experimental scattering spectra from solid-density aluminum. Results are shown from the forward scattering and backward scattering spectrometers with the x-ray beam in seeded and SASE mode of operation. The seeded x-ray beam provides a bandwidth of 1 eV and combined with 8 eV spectrometer resolution resolves the plasmon that is downshifted

from the elastic 8 keV scattering feature by 19 eV. The figure also shows the results of the backward scattering spectrometer which observes elastic scattering at 8 keV reflecting the instrument function of the spectrometer convolved with a Gaussian profile that accounts for the statistical fluctuations of the x-ray energy of a seeded beam over 700 shots.

The experiment with a seeded x-ray laser beam shows that the bandwidth is sufficient to resolve plasmons in dense matter. In forward direction, the x-ray scattering spectra with SASE operation show a slight broadening of red wing of the scattering spectrum but the SASE scattering spectrum is not suitable for inferring the dense plasma conditions.

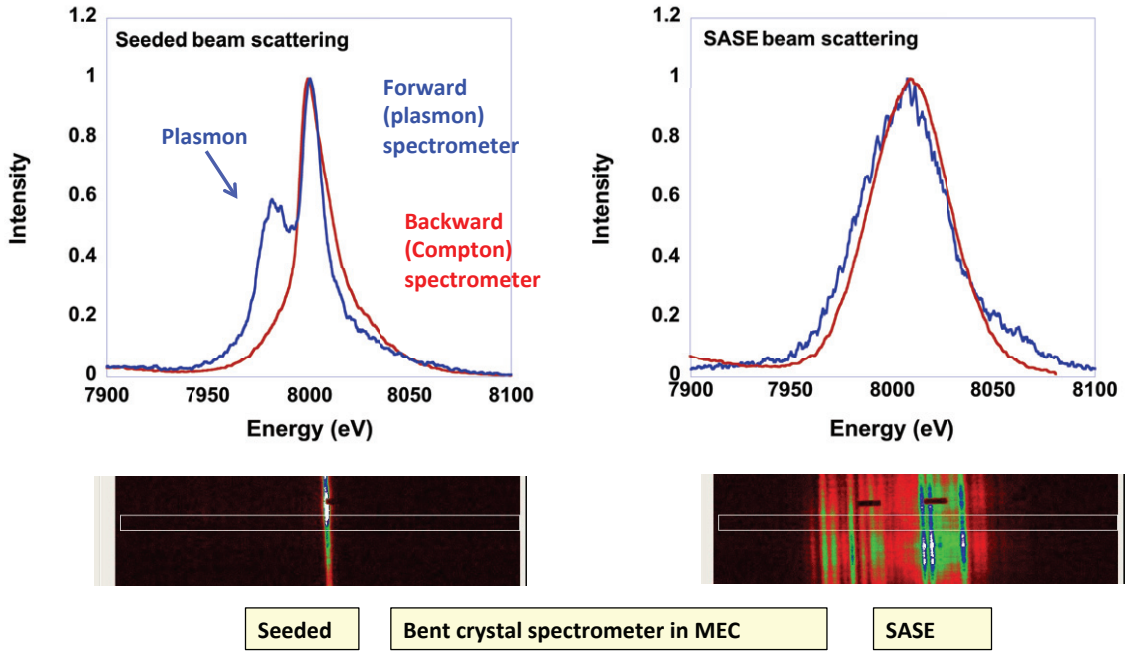

Figure 2. X-ray Thomson scattering data from solid density aluminum targets are shown from forward (plasmon) scattering and backscattering spectrometers for seeded and SASE x-ray beam operation. These data are accumulated over 700 shots at 120 Hz. Also shown are examples of the spectrum of a single x-ray laser shot indicating 1 eV bandwidth for seeded beam and 50 eV for SASE operations.

The backward spectrometer also measured a Compton scattering feature downshifted in energy by 250 eV (not shown). Here, we note that the plasmon resonance is only observed in forward scattering providing strong evidence of a collective phenomenon as predicted for these conditions; bound-free scattering features are predicted to be negligible in this energy range and no feature has been observed with the Compton spectrometer. For these measurements, the crystal in the forward scattering spectrometer is 40 mm thick while in backscattering we employed a 100 mm thick crystal giving rise to slightly different instrument functions and consequently slight differences in the spectral shape of the elastic scattering feature.

When fitting the dynamic structure factor, equation (3) to the experimental forward scattering spectrum we find that the shift of the plasmon peak yields the electron density of $n_e = 1.8 \times 10^{23}$ cm^{-3} ± 5%. The electron temperature is 2 eV accounting for the isochoric heating of the aluminum by the x-ray laser pulse [20]. The ions are cold with temperatures of order 0.1 eV. Here, the plasmon frequency is sensitive to the electron density, but the temperatures are too small to affect the plasmon. The accuracy of the electron density measurement is very high due to the sensitivity of the plasmon

resonance to the plasma frequency. With $n_e = Z/A \, 6.02 \times 10^{23} \rho$ (the electron density n_e in cm^{-3} and the mass density r in g cm^{-3}), assuming ionization state of Z=3 and using the mass A=26.98 u, the measured electron density provides r = 2.7 g cm^{-3} as expected for solid aluminum.

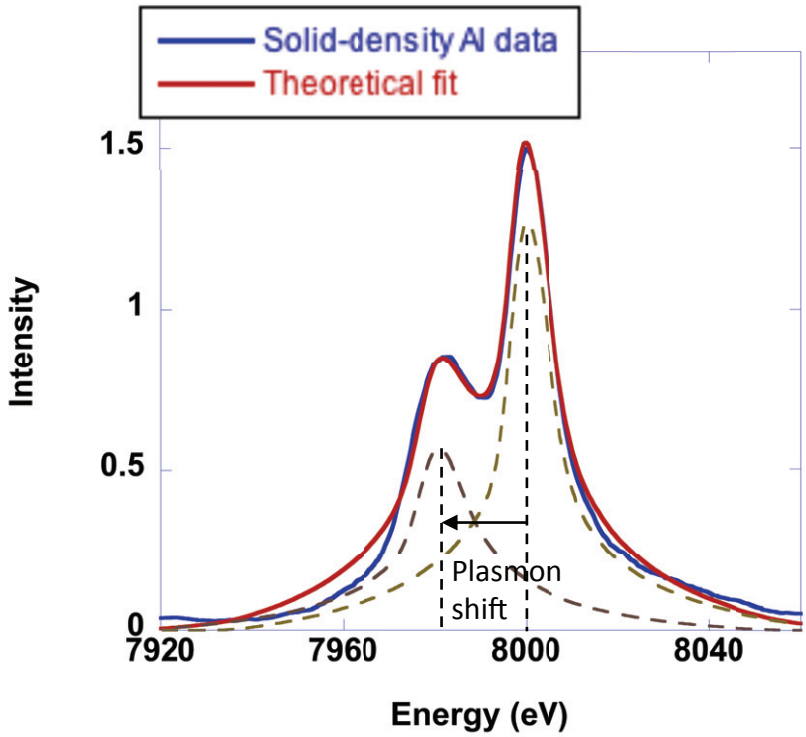

Figure 3. The theoretical fit to the experimental forward X-ray Thomson scattering data is shown for the electron density of n_e = 1.8 x 10^{23} cm^{-3}. The theoretical fit uses an electron temperature of 2 eV reflecting the direct heating of electrons by the x-ray laser interactions. The ions are assumed cold with temperatures of order 0.1 eV. The red dashed curve shows the elastic scattering component and the blue dashed curve represents the plasmon spectrum.

4. Conclusions

With the measurements of plasmon scattering we have demonstrated a highly accurate tool to measure the physical properties of dense matter. This capability is a prerequisite to test predictions of radiation hydrodynamic simulations and density function theory to understand dense matter conditions. Furthermore, the unique combination with pump-probe capability at LCLS will allow novel experiments to discover new phases and material conditions in well-characterized conditions. The high bandwidth and high photon numbers combined with high-resolution crystal spectrometers allows resolving the plasmon shift of 19 eV resulting in an electron density n_e = 1.8 x 10^{23} cm^{-3} ± 5%. This density is consistent with Z=3 in solid aluminum. For future experiments this capability can be applied in single shots to determine, e.g., the conditions of warm dense matter that is compressed by laser-driven shock waves. Also, the technique will allow ultrafast pump-probe studies for measurements of thermodynamic equilibration. On a fundamental level, precision measurements of the plasmon dispersion and amplitude will now be possible. Future developments will include high-resolution spectrometers with sufficient efficiency for measuring the plasmon broadening through Landau and collisional damping processes.

5. References

[1] Emma P, et al. 2010, First lasing and operation of an ångstrom-wavelength free-electron laser, Nature Photonics **4**, 641 - 647.

[2] Lee H J, et al., to be published

[3] Glenzer S H and Redmer R 2009, X-ray Thomson scattering in high energy density plasmas, Rev. Mod. Phys. **81** 1625.

[4] Coppari F et al. 2013, Experimental evidence for a phase transition in magnesium oxide at exoplanet pressures, *Nature Geoscience* doi:10.1038/ngeo1948.

[5] Lindenberg A M et al. 2000, Time-Resolved X-Ray Diffraction from Coherent Phonons during a Laser-Induced Phase Transition, Phys. Rev. Lett. **84** 111.

[6] Fortmann C, Niemann C, and Glenzer S H 2012, Theory of x-ray scattering in high-pressure electrides, Phys. Rev. B **86** 174116.

[7] Glenzer S H et al. 2007, Observations of Plasmons in Warm Dense Matter, Phys. Rev. Lett. **98** 065002.

[8] Kritcher A L et al. 2008, Ultrafast X-ray Thomson scattering of shock-compressed matter, Science **322** 69.

[9] Neumayer P et al. 2010, Plasmons in strongly coupled shock-compressed matter, Phys. Rev. Lett. **105** 075003.

[10] Gregori G and Gericke D O 2009, Low frequency structural dynamics of warm dense matter, Physics of Plasmas **16**, 056306.

[11] Döppner T et al. 2009, Temperature measurement through detailed balance in x-ray Thomson scattering, High Energy Density Physics **5** 182–186.

[12] Amann et al. 2012, Demonstration of self-seeding in a hard-X-ray free-electron laser, Nature Photonics DOI: 10.1038/NPHOTON.2012.180

[13] Lee H J et al. 2009, X-Ray Thomson-Scattering Measurements of Density and Temperature in Shock-Compressed Beryllium, Phys. Rev. Lett. **102** 115001.

[14] Fortmann C et al. 2012, Measurement of the Adiabatic Index in Be Compressed by Counterpropagating Shocks, Phys. Rev. Lett. **108** 175006.

[15] Chihara J 1987, "Difference in x--ray scattering between metallic and non--metallic liquids due to conduction electrons", J. Phys. F: Met. Phys. **17**, 295.

[16] Gregori G et al. 2003, Theoretical model of x-ray scattering as a dense matter probe, Phys. Rev. E. **67,** 026412.

[17] Gregori G et al. 2006, Generalized x-ray scattering cross section from non-equilibrium solids and plasmas, Phys. Rev. E. **74,** 026402.

[18] Zimmerman R 1987, *Many-Particle Theory of Highly Excited Semiconductors* (Teubner, Leipzig).

[19] Thiele R et al. 2008, Plasmon resonance in warm dense matter Phys. Rev. E. **78,** 026411.

[20] Hau-Riege S et al. 2012, Ultrafast Transitions from Solid to Liquid and Plasma States of Graphite Induced by X-Ray Free-Electron Laser Pulses, Phys. Rev. Lett. **108** 217402.

Acknowledgments
This work was performed at the Matter at Extreme Conditions (MEC) instrument of LCLS, supported by the DOE Office of Science, Fusion Energy Science under contract No. SF00515. This work was supported by DOE Office of Science, Fusion Energy Science under FWP 100182, and partially supported by DOE Office of Basic Energy Sciences, Materials Sciences and Engineering Division, under Contract DE-AC02-76SF00515